

Effect of Gravity on the Gelation of Silica Sols

Christine L. Pienaar,[†] Gwenaél J. A. Chiffolleau,[§] Lana R. A. Follens,^{||} Johan A. Martens,^{||}
Christine E. A. Kirschhock,^{*||} and Theodore A. Steinberg[‡]

Defence Science and Technology Organisation, Edinburgh South Australia, Australia, Phenomena in μ -Gravity Laboratory, School of Engineering Systems, Faculty of Built Environment & Engineering, Queensland University of Technology, Brisbane, Queensland, Australia, Wendell Hull & Associates, Inc., Las Cruces, New Mexico 88005, and Centre for Surface Chemistry and Catalysis, Katholieke Universiteit Leuven, Kasteelpark Arenberg 23, B-3001 Leuven, Belgium

Received December 9, 2005. Revised Manuscript Received December 4, 2006

Acid-catalyzed silica polymerization was carried out under gravity conditions varied from 0.01 g aboard a reduced gravity aircraft to 70g in a centrifuge. The silicate connectivity of the final xerogels was analyzed using solid state ²⁹Si NMR and the porosity using nitrogen adsorption. Gravity was found to have an important influence on the occurrence of intra- and intermolecular condensation reactions. Under reduced gravity buoyancy driven-free convection is limited and silica polymerization occurs in a diffusion-limited regime. Intramolecular condensations and densifications prevail and extended coils of cages are formed through cyclization reactions in the sol particles. In terrestrial and high-gravity conditions, bimolecular reactions compete more favorably with internal condensations. More open structures composed of chains and rings are formed. These flexible species delay the onset of gelation, leading to an increase in gelation time as the gravity level is increased. During the subsequent drying procedure, pore collapse changes the structure from meso- to microporous. The porosity of the finally obtained xerogels is mostly defined by the drying conditions of the gel, irrespective of the silicate connectivity.

Introduction

The sol–gel process^{1–3} is a low-temperature materials production process combining benefits from glass and plastics technology.⁴ Utilized since the 1930s,⁵ reaching a peak in research in the 1980s,^{3,6–9} it is currently applied in a vast array of research disciplines,¹⁰ including the billion dollar nanomaterials industry.^{4,11,12} Acid-catalyzed silica sol–gel processes are used, e.g., to produce xerogels, which find applications in high-temperature ceramics, thermally isolating coatings, molecular filtration, and thin film sensors.^{4,10,13}

It has been stated that “a critical hurdle in the development of sol–gel techniques for the preparation of inorganic materials is elucidating the effect of key synthesis and

processing parameters on the structure of the resulting sols”.¹⁴ One such poorly understood parameter is gravity, despite reduced gravity research being conducted on the formation of glass–metal composites,¹⁵ sol–gel-derived zeolites,¹⁶ colloidal aggregation of silica,¹⁷ growth rates in silicon,¹⁸ oxide glasses,¹⁹ and silicate gardens.²⁰ Smith et al.²¹ and Snow et al.²² established that a reduction in gravity had a profound effect on the growth of silica nanoparticles formed by the sol–gel method. Those authors reported that the current understanding of the formation of the molecular structure failed to address the influence of primary silica species and their aggregates in the sol. The impact of gravity on the aggregation of larger species, like colloidal hard silica spheres, also has been demonstrated.²³ However, to our knowledge, there has been no high gravity research conducted in the area of polymeric acid-catalyzed silica sol–gel processes.

* To whom correspondence should be addressed. E-mail: christine.kirschhock@biw.kuleuven.be.

[†] Defence Science and Technology Organisation.

[‡] Queensland University of Technology.

[§] Wendell Hull & Associates.

^{||} Katholieke Universiteit Leuven.

- (1) Wright, J.; Sommerdijk, N. *Sol-gel Materials: Chemistry and Applications*; Taylor & Francis Books, Ltd.: London, 2001.
- (2) Brinker, C. J.; Scherer, G. W. *Sol-Gel Science: The Physics and Chemistry of Sol-Gel Processing*; Academic Press: San Diego, 1990.
- (3) Hench, L.; West, J. *Chem. Rev.* **1990**, *90*, 33.
- (4) Wilson, M.; Kannangara, K.; Smith, G.; Simmons, M.; Raguse, B. *Nanotechnology: Basic Science and Emerging Technologies*; UNSW Press: Melbourne, 2002.
- (5) Hurd, C. *Chem. Rev.* **1938**, *22* (3), 403.
- (6) Pope, E.; Mackenzie, J. J. *Non-Cryst. Solids* **1986**, *87*, 185.
- (7) Pope, E.; Mackenzie, J. J. *Non-Cryst. Solids* **1988**, *101*, 198.
- (8) Ulrich, D. J. *Non-Cryst. Solids* **1988**, *100*, 174.
- (9) Kay, B.; Assink, R. J. *Non-Cryst. Solids* **1988**, *104*, 112.
- (10) Pope, E. *Key Eng. Mater.* **1998**, *150*, 141.
- (11) Hsiao, J.; Fong, K. *Nature* **2004**, *428*, 218.
- (12) Cyranoski, D. *Nature* **2000**, *408*, 624.
- (13) Tulloch, G.; Tulloch, S. *Key Eng. Mater.* **1998**, *150*, 185.

- (14) Meixner, D. L.; Gilicinski, A. G.; Dyer, P. N. *Langmuir* **1998**, *14*, 3202.
- (15) Korwin, M.; Lynch, K.; LaCourse, W. *Ceram. Eng. Sci. Proc.* **1999**, *20* (4), 251.
- (16) Warzywoda, J.; Bac, N.; Jansen, J.; Sacco, A. *J. Cryst. Growth* **2000**, *220*, 140.
- (17) Okubo, T.; Tsuchida, A.; Kobayashi, K.; Kuno, A.; Morita, T.; Fujishima, M.; Kohno, Y. *Colloid Polym. Sci.* **1999**, *277*, 474.
- (18) Schweizer, M.; Croll, A.; Dold, P.; Kaiser, T.; Lichtensteiger, M.; Benz, K. J. *Cryst. Growth* **1999**, *203*, 500.
- (19) Inoue, S.; Makishima, A.; Inoue, H.; Soga, K.; Konishi, T.; Asano, T. *J. Non-Cryst. Solids* **1999**, *247*, 1.
- (20) Jones, D.; Walter, U. *J. Colloid Interface Sci.* **1998**, *203*, 286.
- (21) Smith, D.; Sibille, L.; Cronise, R.; Hunt, A.; Oldenburg, S.; Wolfe, D.; Halas, N. *Langmuir* **2000**, *16*, 10055.
- (22) Snow, L.; Smith, D.; Sibille, L.; Cronise, R.; Ng, J.; Halas, N.; Hunt, A. *Polym. Prepr.* **2000**, *41* (1), 1062.
- (23) Zhu, J.; Li, M.; Rogers, R.; Meyer, W.; Ottewill, R.; Russel, W.; Chaikin, P. *Nature* **1997**, *387*, 883.

Initially, in an acid-catalyzed sol–gel process departing from silicon alkoxide with sufficient water-to-silica ratio, silicate monomers are formed through hydrolysis and dominate the distribution of siliceous species. At later stages, condensation reactions convert the silanol groups, Si–OH, to siloxane bonds, Si–O–Si. Condensations can be through bimolecular reactions, which contribute to particle growth, or through intramolecular cyclization reactions, which result in the formation of rings and cages.

The importance of cyclization during silica growth has been demonstrated.^{24–27} The small size of silica chains and the flexibility of siloxane bonds imply small rings can easily form during ordinary alkoxy silane condensation.²⁴ Even in highly branched systems, cyclization can still occur through backbiting and chain pinching. The present work documents, for the first time, that gravity has a direct impact on the degree of cyclization during silica sol–gel processes. Gravity influences the extent and type of cyclization which occurs during structural growth and thus, as a result, gravity ultimately determines the final structure of silica sol–gel materials.

Experimental Methods

Sample Synthesis. The xerogel was formed from a silicate-based, acid-catalyzed sol, composed of ethanol, 20 mL of tetraethylorthosilicate (TEOS), and 20 mL of stock solution. The stock solution was a mixture of 1 mL of 1 M nitric acid with 800 mL of reverse osmosis treated water. The silica sol, referred to as the parent sol, was synthesized inside a water bath maintained between 0 and 4 °C to prevent premature gelation. A parent sol was prepared by dropwise addition of stock solution to the mixture of TEOS and ethanol under continuous stirring. The parent sol was then heated to 60 °C for 90 min before being cooled to room temperature and diluted 2:1 on a volume basis with ethanol. The final molar ratio of the parent sol was 1:26.76:12.37:0.015 TEOS:ethanol:water:nitric acid.

Apparatuses. Two experimental apparatuses were built. A reduced gravity apparatus (RGA) constructed within strict NASA guidelines was used to conduct reduced gravity experiments aboard NASA's KC-135 Reduced Gravity Aircraft, which provides (10^{-2} – 10^{-4})g for 25 s. Due to this time constraint, it was necessary to speed up the gelation process by simultaneously heating the sol and exposing it to a vacuum. Therefore, the RGA consisted of a molecular drag pump backed by two twin-head diaphragm pumps, supplying a vacuum level to 1×10^{-5} Torr with a 1 m³/h pump rate. A buffer tank was used to increase the rate at which pressure within the apparatus was decreased. A connector allowed easy detachment and reattachment of experimental sections in preparation for the next reduced gravity parabola. The RGA was capable of being coupled to the centrifuge to allow reference experiments under normal gravity as well as increased gravity levels. The high-gravity apparatus (HGA) consisted of an oil-lubricated pump capable of 0.45 Torr, with a 7.5 m³/h pumping rate, connected to a centrifuge, which could produce up to 70g. Again the sol was heated to between 50 and 60 °C. To assess the influence of evacuation during gelation,

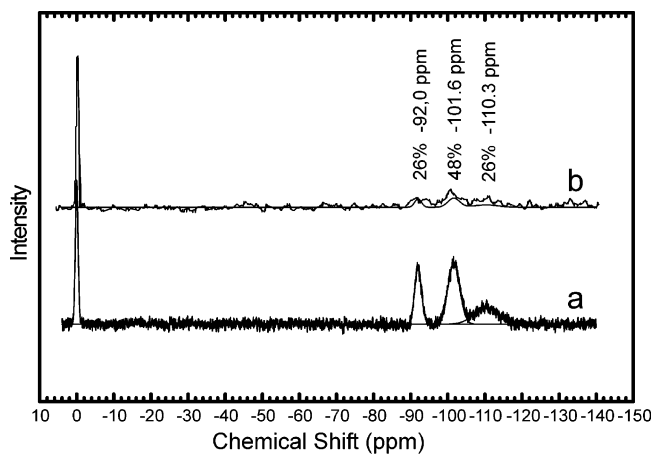


Figure 1. Liquid NMR spectra showing moieties present in parent sol (a) after 90 min of heating at 60 °C and after shorter heating times (b). The low-intensity results from short measurement times to ensure no change in the connectivity occurred during measurement. Also shown is the fitted Q ratio of the spectra. The stability of the sol during and after dilution was verified with DLS measurements (not shown).

control samples were synthesized at the same gelation temperature but under ambient pressure. Except for the microgravity experiments all syntheses were repeated several times to ensure reproducibility. All tests were conducted with 2 mL of sol.

Sample Characterization. Liquid NMR was used to determine which chemical species were present in the parent sol. ²⁹Si liquid NMR was performed on a Bruker AMX 300 MHz (7 T) at 0 °C. Tetramethylsilane (TMS) was used as chemical shift reference. Peak assignments were made according to previously published results.²⁸ DLS measurements were performed on an ALV-NIBS particle sizer in backscatter mode.

The silicate connectivity of the dry samples was determined using solid-state NMR (²⁹Si MAS NMR). The Qⁿ functional group terminology (*n* refers to the number of Si–O–Si bonds of the corresponding silicon atom) was adopted. A Bruker MSL 300 at a ²⁹Si frequency of 59.627 MHz with standard pulse sequence was used. The ²⁹Si 90° pulse time was 4.0 s. Spectra were collected with high-power decoupling of the ¹H nuclei, allowing for a pulse repetition time of 20 s. The samples were spun at the magic angle within the Bruker 4 mm MAS probe with spinning speed of 3–4 kHz. The acquisition time was 34 ms. Chemical shifts are relative to TMS via the higher chemical shift peak of kaolinite, which lies at –91.03 ppm. The NMR spectra summary (Table 2, examples of deconvoluted peaks in Figure 3), shows the Qⁿ ratio obtained by fitting of the spectra with Gauss-Lorentz curves. Regression ratios were 0.99 or better. Samples synthesized under identical conditions to ensure reproducibility varied in Q ratio less than 2%.

An Autosorb-1 by Quantachrome Instruments was used for determining nitrogen adsorption/desorption isotherms at –196 °C. The specific surface area was determined using the Brunauer–Emmett–Teller (BET) equation. Samples were degassed overnight and heated to 200 °C for the first 4 h of degassing. The microporous samples were analyzed using the SF method.²⁹ Cylindrical micropore morphologies were assumed, which is supported by the consistent absence of hysteresis effects in ad- and desorption. Samples synthesized under identical conditions to ensure reproducibility varied in pore volume <10%.

For the nitrogen adsorption and ²⁹Si NMR tests, most samples were analyzed within 2 weeks of formation. However, for the

(24) Rankin, S.; Kasehagen, L.; McCormick, A.; Macosko, C. *Macromolecules* **2000**, *33*, 7539.

(25) Rankin, S.; Macosko, C.; McCormick, A. *Chem. Mater.* **1998**, *10*, 2037.

(26) Ng, L.; McCormick, A. *J. Phys. Chem.* **1996**, *100*, 12517.

(27) Ng, L. V.; Thompson, P.; Sanchez, J.; Macosko, C. W.; McCormick, A. V. *Macromolecules* **1995**, *28*, 6471.

(28) Pouxviel, J.; Boilot, J.; Beloeil, J.; Lallemand, J. *J. Non-Cryst. Solids* **1987**, *89*, 345.

(29) Saito, A.; Foley, H. *Microporous Mater.* **1995**, *3*, 531.

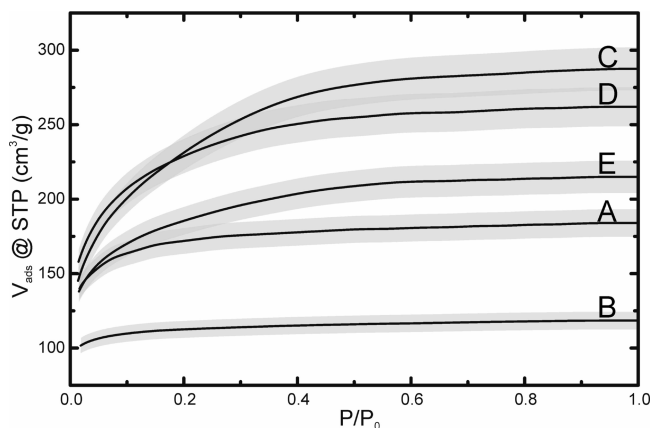


Figure 2. Nitrogen adsorption isotherms at $-196\text{ }^{\circ}\text{C}$. Gray areas indicate the worst possible deviation ($\pm 5\%$) between samples synthesized under identical conditions. Sample C: Sample formed and gelled in reduced gravity and dried under normal gravity and ambient conditions. Sample D: Sample formed and gelled in terrestrial gravity and dried under normal gravity and ambient conditions. Sample E: Sample formed, gelled, and dried in a $50\text{ }^{\circ}\text{C}$ oven (RGA not used). Sample A: Reduced gravity apparatus used and sample formed, gelled, and dried at 2g , vacuum and heating. Sample B: High-gravity apparatus used and sample formed, gelled, and dried at 2g , vacuum and heating.

reduced gravity sample, isotherm and NMR spectra were not obtained until 3 months after the NASA tests were completed in the United States. Repetition of the solid-state MAS NMR measurements of the samples as a function of time ensured that the structure of a dry sample does not change significantly post formation. It was found that samples as old as 6 months had not aged appreciably.

Results and Discussion

Characterization of the Parent Sol. ^{29}Si Liquid NMR spectra were collected during synthesis of the parent sol, shortly after addition of the acid catalyst and after different times of reflux heating at $60\text{ }^{\circ}\text{C}$ (Figure 1). Shortly after addition of the acid catalyst the parent sol contains partially and fully hydrolyzed monomers next to TEOS. The liquid still appeared slightly turbid due to incomplete hydrolysis. After heating for 15 min the liquid turned fully transparent as TEOS was fully hydrolyzed, no unhydrolysed TEOS, or even monomeric silica was observed (Figure 1b). Over the following 75 min of heating the Q ratio in the sample did not significantly change (Figure 1a). The NMR signals are significantly broadened due to the already achieved size and/or broad distribution of chemical environments of the formed silica species. After 90 min of heating the sample shows a $\text{Q}^2:\text{Q}^3:\text{Q}^4$ ratio of 26:48:26. The significant broadening of the signals (Figure 1a) indicates that already at this stage larger species, hindered in mobility, have formed. A DLS study of this sample revealed characteristic sizes of silica species of 16 nm, explaining the broadening. When an undiluted sol was left for 1 week, the onset of gelling was observed by DLS. It is known from literature that dilution of a sol with ethanol prevents premature gelling.^{2,30,31} Indeed, when the sol was diluted directly after heating, the characteristic particle size of 16 nm was retained over longer

Table 1. List of Samples

name	test gravity and test time	apparatus	state at collection	gelation conditions	drying conditions
A	2g 30 min	RGA	powder	2g $\sim 50\text{ }^{\circ}\text{C}$ vacuum	2g $\sim 50\text{ }^{\circ}\text{C}$ vacuum
B	2g 15 min	HGA	powder	2g $\sim 50\text{ }^{\circ}\text{C}$ vacuum	2g $\sim 50\text{ }^{\circ}\text{C}$ vacuum
C	reduced 25 s	RGA	gel	<1g $\sim 50\text{ }^{\circ}\text{C}$ vacuum	1g ambient T atm. P
D	terrestrial 70 s	RGA	gel	1g $\sim 50\text{ }^{\circ}\text{C}$ vacuum	1g ambient T atm. P
E (control)	terrestrial 3 h	Oven	powder	1g $50\text{ }^{\circ}\text{C}$ atm. P	1g $50\text{ }^{\circ}\text{C}$ atm. P
F	terrestrial 15 min	HGA	powder	1g $\sim 50\text{ }^{\circ}\text{C}$ vacuum	1g $\sim 50\text{ }^{\circ}\text{C}$ vacuum
G	70g 15 min	HGA	powder	70g $\sim 50\text{ }^{\circ}\text{C}$ vacuum	70g $\sim 50\text{ }^{\circ}\text{C}$ vacuum

periods (up to 2 weeks). This stabilized parent sol could therefore be stored for at least a week, without noticeable change.

Influences of Gravity and Drying Conditions on Silicate Condensation. In the sol–gel experiments, 2 mL aliquots of sol were heated in vacuo at different gravity levels. Test times were varied, with some tests halted when the sol gelled. Longer test times produced dry powders. Irrespective of the state of the sample at completion of the test, whether gel or powder, the sample was placed in 20 mL open bottles and left to dry under ambient conditions under normal gravity. The final outcome was a set of powder samples which could be analyzed using nitrogen adsorption (Figure 2) and solid-state ^{29}Si NMR (Figure 3). Table 1 summarizes the samples analyzed in this paper. The Q^n connectivity and the porosity of the samples are reported in Table 2.

Two different experimental setups with different pumping characteristics were used: HGA and RGA. It had to be ensured that both apparatuses resulted in identical samples under similar experimental protocols. This was achieved by comparison of samples A (obtained in RGA) and B (obtained in HGA) where the sol–gel reactions in vacuo heating and 2g conditions yielded dry powder products. The ^{29}Si MAS NMR spectra for samples A and B show a similar distribution of Q^2 , Q^3 , and Q^4 groups (Table 2). Hence the degree of condensation inside the xerogel was independent of the pumping rate and vacuum level of the two apparatuses. This indicates samples obtained in the two setups can be directly compared regarding the connectivity of the silica.

The RGA was used to perform the sol–gel process in reduced gravity aboard the aircraft and on ground under terrestrial gravity. As the reduced gravity test time was too short to obtain powders, the obtained gel was left to dry under ambient temperature and pressure at 1g . Control sample E (1g) was gelled and dried at $50\text{ }^{\circ}\text{C}$ in an oven under atmospheric pressure. Sample D was prepared within 70 s using the RGA apparatus under terrestrial gravity and then

(30) Buckley, A.; Greenblatt, M. *J. Non-Cryst. Solids* **1992**, *143*, 1.

(31) Rodriguez, R.; Arroyo, R.; Salinas, P. *J. Non-Cryst. Solids* **1993**, *159*, 73.

Table 2. Results of Porosimetry and MAS Solid State ^{29}Si NMR Data^a

name	gravity level	apparatus	A_s (m ² /g)	D (nm)	V (cm ³ /g)	Q^2 (%) (ppm peak center)	Q^3 (%) (ppm peak center)	Q^4 (%) (ppm peak center)
A	2g	RGA	625.7	1.8	0.28	6.6 (-92.6)	53.1 (-102.0)	40.2 (-111.4)
B	2g	HGA	405.9	1.8	0.18	5.6 (-91.9)	51.7 (-102.0)	42.7 (-111.4)
C	reduced	RGA	834.5	2.1	0.44	0.85 (-88.3)	31.7 (-99.6)	67.5 (-113.9)
D	terrestrial	RGA	834.5	1.9	0.41	6.1 (-92.6)	45.0 (-102.2)	48.9 (-111.1)
E	control	oven	672.2	2.0	0.33	5.6 (-92.6)	46.5 (-102.0)	47.9 (-111.4)
F	terrestrial	HGA	406.3	1.8	0.19	5.3 (-92.1)	46.4 (-102.0)	48.2 (-111.3)
G	70g	HGA	350.5	1.8	0.16	5.1 (-92.4)	51.6 (-102.0)	43.3 (-111.5)

^a A_s : surface area; D : average pore diameter; V : total pore volume.

allowed to dry at ambient conditions. Samples E (control, 1g) and D (RGA, 1g) had almost identical Q^n ratios, despite control sample E being formed in an oven and D in vacuo until it gelled. Thus, the presence of a vacuum during gelation had no effect on the final molecular connectivity in the xerogel. This is in line with the observation that the different vacuum systems in HGA and RGA have negligible effect on the Q^n ratio in the samples. Another observation results from comparison of samples D, E, A, and B: Once the samples have reached the gel state, neither drying temperature nor evacuation during drying had any significant effect on the Q^n ratio of silicon atoms in the network. Therefore, comparison of Q^n ratios irrespective of drying conditions readily gives insight into the molecular connectivity at the gel point.

Sample C was prepared under similar conditions as sample D, but gelation occurred under reduced gravity conditions. In comparison to sample D it contained higher levels of Q^4 groups, less Q^3 groups, and practically no Q^2 groups (Table 2). With use of the Q^n ratio of the product as a marker for connectivity in the gel state, sample A (RGA; 2g) showed the opposite trend, less Q^4 and more Q^3 groups than samples C and D which were obtained at lower gravity.

The HGA was used to create xerogels under 1, 2, and 70g (Table 2). It is clear that the higher gravity samples (sample B, 2g; sample G, 70g) had less Q^4 groups and more Q^3 groups than the 1g sample F. Interestingly, samples B and G had identical Q^n group ratios. It was also observed that the time to reach the gel point increased with increasing gravity.³² This effect seems directly linked to the degree of condensation of the molecular species directly before gelling.

Influence of Gravity and Drying Conditions on Silica Xerogel Texture. Despite the presence of similar Q^n group ratios (Table 2), sample B formed with the HGA (i.e., faster pumping rate) had a lower specific surface area and less pore volume than sample A formed with the RGA (i.e., slower pumping rate). These results show that while the pumping rate did not affect the molecular connectivity of the xerogel, it did affect the degree of pore collapse upon drying (Table 2). Faster evaporation resulted in loss of porosity, an effect also reported by other researchers.^{33,34} The marked effect of

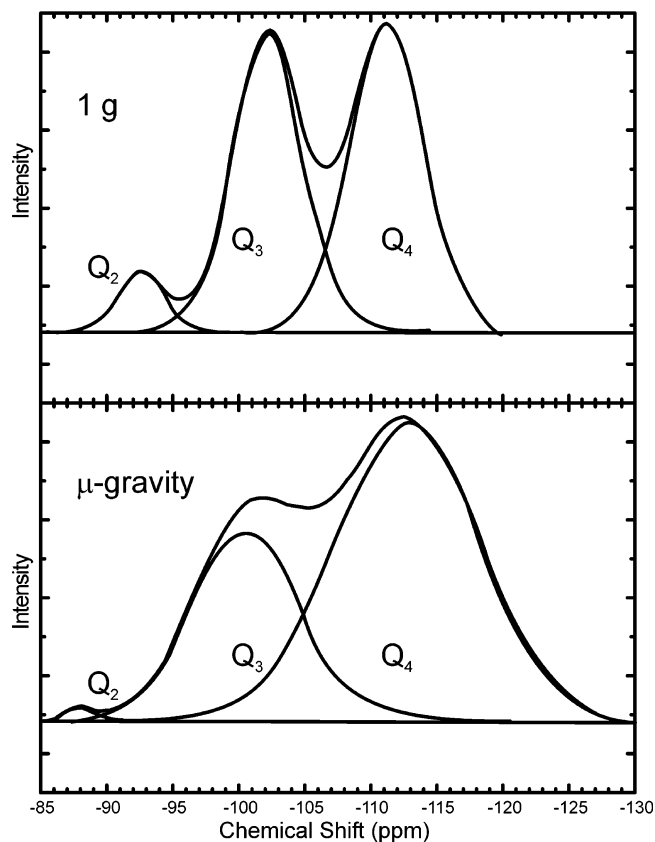


Figure 3. Examples of deconvoluted peaks from ^{29}Si NMR. Top: Sample D: Reduced gravity apparatus used and sample formed and gelled in normal gravity. Bottom: Sample C: Reduced gravity apparatus used and sample formed and gelled in reduced gravity.

the drying rate on the samples' porosity was observed with the other samples too. Control sample E was heated to 50 °C during drying and, therefore, dried more quickly than sample D which dried at ambient temperature. Sample E had a lower surface area and lower total pore volume compared to sample D (Table 2). This means elevated temperatures during the transition from alco-/hydrogel to xerogel have a similar effect as increased pumping rates, resulting in partial pore collapse.

Samples C and D were dried under similar ambient conditions. Despite these strong differences in Q^n distribution (Table 2, Figure 3), porosity and specific surface area of the two samples are almost identical (Table 2, Figure 2). This again clearly shows that the drying procedure defines the final porosity in a more pronounced way than the Q^n ratio of the gel. Sample A has a lower surface area and pore volume than samples C and D, due to evacuation during the drying step. Finally, B, G, and F are samples that experienced identical drying procedures. Nitrogen adsorption reveals that specific surface area and pore volume of these three samples is very similar, despite strong differences in the Q^n distributions caused by differences of gravity conditions during gelation. Sample G, subjected to 70g, showed a slight decrease of porosity, most probably due to pore collapse as a result of mechanical stress. In summary, the porosity of

(32) Pienaar, C.; Lu, G.; Steinberg, T.; da Costa, J. *Nanomater. Res. Conf.* **2004**, 27.

(33) Dumas, R.; Tejedor-Tejedor, I.; Anderson, A. J. *Porous Mater.* **1998**, 5, 95.

(34) Huang, W.; Cui, S.; Yuan, Z.; Liang, K. *Physica A* **2002**, 312, 70.

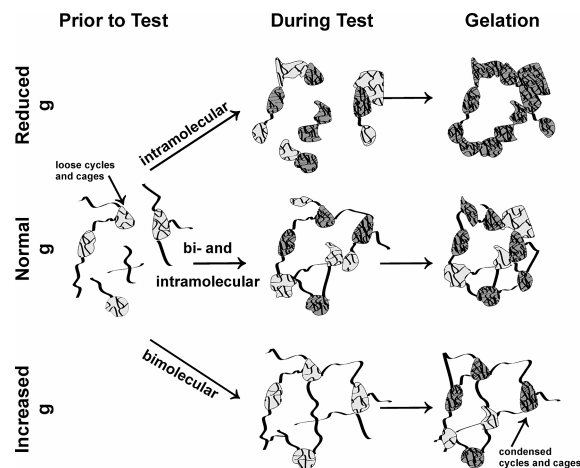


Figure 4. Growth of molecular structures in various gravity regimes. In reduced gravity a diffusion-limited regime results in domination of intramolecular cyclization. The cyclic building units then react with their nearest neighbors, leading to extended coils of cages and a structure high in Q^4 groups at gelation. In normal and high gravity, diffusion allows bimolecularization to compete with cyclization, resulting in a mixture of chains as well as cycles.

the xerogels is entirely defined by the post-treatment after gelation, irrespective of the silicate connectivity in the gels.

Impact of Gravity on Silica Condensation Pattern.

Bringing the data together, the model shown in Figure 4 explains the effect of gravity on the sol–gel process. Silica polymers grow through bimolecular reactions. In the pH range 2–7 it is established that the preferred reaction is between species of high and low molecular weight.⁴ Internal condensation reactions give rise to the formation of cycles with three or more silicon atoms in a ring. Such rings are obtained when silicate groups on chain ends react with central groups on the same chain.^{25–27} If dilution levels are high or if the movement of the molecular species is restricted, then cyclization is dominant.²⁶ Reaction between polymer chains is possible only if sufficient mobility exists.²⁶ The bimolecular collision frequency has to be higher than the intramolecular cyclization rate for chains to grow in favor of cycle formation. The parent sol was composed mainly of stable loosely interconnected cycles as evidenced by the liquid NMR and DLS study.

Under the experimental conditions used in this work, heating the 2 mL sample of sol at 50 °C and evacuation of ethanol and water both promoted condensation reactions. The ²⁹Si NMR data revealed that, under reduced gravity, a high level of Q^4 groups was created within a short time (Table 2). This high Q^4 content indicates that highly condensed silica species were present at the point of gelation. Upon removal of solvents, the initial silica species intramolecularly densified because the lack of buoyancy driven free convection suppressed intermolecular condensation. These highly condensed and therefore rather rigid species could rapidly gelate as soon as the solvent content dropped below a threshold where silica species started to interact with each other.

In terrestrial and elevated gravity environments, buoyancy driven convection lifted mass transport limitations and rendered bimolecular reactions to effectively compete with intramolecular densification. Higher gravity levels are equivalent to larger and less dense species forming due to higher

bimolecular collision rates. Just before gelation the mixture was dominated by long, branched chains separating the cycles. The curious observation that the degree of condensation only increased slightly between 2 and 70g can be explained by an increased condensation rate, once sufficiently long and branched species are formed through bimolecular condensation reactions. Combined with the decreased probability of collisions between molecules once the smaller entities are depleted, this limits the average length of Q^2 sequences and results in a minimum amount of Q^4 silicon content, around 43% in the system studied. During gelling a very open, rather unstable network was formed which needed cross-linking to attain a gelled state. This necessary densification step resulted in a molecular structure which contained condensed cycles next to chains, as mirrored in the observed Q^n distributions. The required rearrangement and flexibility of chains accounted for the increase in gel times, which were observed at higher gravities. In reduced gravity the molecular species before gelation consisted of cycles, contained in cages and coils, which were stabilized by intramolecular hydrogen bonds.³⁵ These already highly condensed species gelled once the smaller moieties (Q^2) were depleted.

Conclusions

The silica condensation pattern in acid-catalyzed sol–gel processes was investigated under varying gravity levels. In reduced gravity a completely new connectivity in the obtained xerogels was observed. Between 2 and 70g the molecular structure was identical. A reduction in gravity reduced buoyancy driven free convection, leading to a diffusion-limited silica polymerization process. This regime favored intramolecular cyclization and suppressed bimolecular condensation reactions which require mobility of molecules. As a result, in reduced gravity the molecular structure grew through the condensation of coils, cycles, and cages into a highly condensed gel. The Q^4 groups present in the structure were stabilized due to their cyclic configuration. The coiled structures condensed easily into a gel. In terrestrial and high gravity, bimolecularization reactions competed with cyclization to form a structure composed of chains and cycles. This structure was more open and unstable, requiring rearrangement of the chains and cycles for gelation to occur. The flexibility imparted by chains in the structure resulted in increased gelation times.

Acknowledgment. Testing aboard the KC-135 was made possible by contributions from NASA White Sands Test Facility's Laboratory Department in New Mexico and the NASA Johnson Space Center in Texas. Thanks and appreciation is also extended to Dr. A. Whittaker from the Centre for Magnetic Resonance and to Professor J. Drennan and Mr. J. Nailon from the Centre for Microscopy and Microanalysis, all at the University of Queensland. Partial financial support was provided by the Australian Research Council and University of Queensland through the ARC Centre for Functional Nanomaterials. The Belgian Government is acknowledged and thanked for supporting an interuniversity pole of attraction (IPA-PAI). C.E.A.K. and J.A.M. acknowledge financial support by ESA and the Belgian Prodex office.

CM0527219